Beam Selection in Angle Diversity MIMO Systems for Optical Wireless Systems

Janis Sperga
Department of Electronic & Electrical Engineering
University of Strathclyde
Glasgow G1 1XW, U.K
Email: janis.sperga@strath.ac.uk

Rui Bian
pureLiFi Ltd
Edinburgh EH12 5EZ, U.K.

Harald Haas
LiFi Research and Development Centre
University of Strathclyde
Glasgow G1 1RD, U.K.
Email: harald.haas@strath.ac.uk

***Abstract*—Energy efficiency is one of the main benchmarks of performance in visible light communication. Achieving high energy efficiency in a link is a challenging task when high data throughput is required. A promising approach to tackling this challenge is using multiple-input-multiple-output (MIMO) systems, which use the spatial domain for information encoding. A novel modulation scheme called Flexible light emitting diode (LED) index keying (FLIK) can harness high spectral efficiency by utilising active and inactive LED states. The high spectral efficiency, together with a straightforward encoding, makes FLIK based design a promising candidate for high energy efficiency and data throughput solutions. However, the system's performance based on FLIK depends heavily on beam selection participating in the link, which can significantly vary with the channel conditions subject to the user's position and orientation. In a dynamic use case scenario, a fast beam selection and selection re-adjustment are vital for an optimal use case. This study examines the performance of beam selection based on a maximal signal-to-noise ratio (SNR) criterion in angle diversity hemispherical transceiver systems. In this paper, a random orientation system model for FLIK is considered. The simulations are then performed considering maximal SNR and maximal Euclidean distance criteria. The performance is evaluated in terms of achievable data throughput. A selection method, based on the maximal SNR, is compared to a method based on maximising Euclidean distance. The numerical results show that for both the fixed and random orientation cases, a beam selection based on maximal SNR performs as well as the one based on Euclidean distance. This observation is valid up to 25 degrees of beam half-intensity angle, therefore, validating the use of maximal SNR condition in such systems.**

***Index Terms*—Visible light communication (VLC), Multiple-input-multiple-output (MIMO) systems, LiFi, Flexible LED Index Keying (FLIK), Beam selection, device orientation.**

I. Introduction

The Ericsson mobile data traffic forecast has reported that up to 49 EB (exabytes) of data traffic was generated monthly at the end of 2020 and is projected to grow nearly 5-fold to reach 237 EB per month in 2026 [1]. The ever increasing data traffic is followed by growing energy consumption. It has been estimated in [2] that ICT (information & communication technology) accounts for 5-9% of global energy consumption and 2% global CO2 emissions around the same amount as the fuel emissions from the whole aviation industry [3].

This calls for further innovation in the field of wireless communications. Visible light communication (VLC) has emerged as alternative source of new innovation to the contemporary RF wireless technologies offering a vast and unregulated 300 THz available light spectrum [4]. A fully networked mobile VLC bi-directional multi-user system is called LiFi (short for light-fidelity) [5].

However, to fully emerge as a viable market alternative to the next-generation of wireless technologies with ever stringent energy-saving requirements, LiFi based technology should adhere to green design principles requiring the development of energy-efficient system designs that are at least as efficient as the RF-based ones [6].

For high data rate solutions, meeting the energy efficiency requirements becomes a challenging task. A promising method to achieve energy efficiency while keeping a high data throughput is to harness spatial multiplexing gains using (MIMO) transmission techniques that utilise multiple transmitters and receivers participating in the link [7].

MIMO systems based on the spatial/angle diversity modulation schemes (e.g., Spatial Modulation (SM) [8], Generalised Space Shift Keying (GSSK) [9], Flexible LED Index Modulation (FLIM) [10]) promise potentially more energy-efficient and less computationally complex high data rate design solutions compared to the solutions based on multi-carrier modulation schemes.

Nevertheless, an appropriate, adaptive fast beam selection method is required to properly implement and harness these modulation schemes in a mobile use case scenario. Generally, such methods can be based on optimal selection methods for maximising the Euclidean distance between symbols [11] or by selecting beams that maximise link SNR [12].

In this paper, we apply beam subset selection based on the maximal SNR criterion for an angle diversity hemispherical system using a special sub-type of FLIM called Flexible LED index keying (FLIK). We compare the method's performance to one using the Euclidean distance method as a selection criterion in a dynamic use case scenario where the user equipment (UE) is free to have an arbitrary position and orientation relative to the access point (AP).

The rest of the paper is organized as follows. Section II describes the random orientation model for FLIK. Section III presents the angle diversity hemispherical transceiver model and gives optical test setup parameters for simulations. Section

This is a peer-reviewed, accepted author manuscript of the following paper: Sperga, J., Bian, R., & Haas, H. (2022). Beam selection in angle diversity MIMO systems for optical wireless systems. In 2022 IEEE International Conference on Communications Workshops (ICC Workshops) (pp. 445-450). IEEE. https://doi.org/10.1109/iccworkshops53468.2022.9814683

IV revolves around computer simulation results, and the paper is drawn to the conclusion in Section V.

Notation: Italic symbols denote scalar values, matrices and column vectors are denoted with bold uppercase and lowercase letters respectively. We use $(\cdot)^{\mathrm{T}}$ for transpose. In this study index j will refer to the AP elements (LED cells), while i to the UE elements (receiver cells). $|\cdot|_{\mathrm{F}}$ is Frobenius norm. Real Gaussian distribution with a mean μ and variance σ^2 is symoblized by $\mathcal{N}(\mu, \sigma^2)$. Dot product, argument maximum and minimum, rectangular function, a set and its cardinality is given as follows: $\cdot$, $\arg\max$, $\arg\min$, $\mathrm{rec}(\cdot)$, $\mathbb{A}$, $|\mathbb{A}|$.

II. Random Orientation in FLIK

In the following, we will briefly outline FLIK and introduce a random orientation system model in an angle diversity hemispherical transceiver system. We will briefly describe beam selection criteria.

A. FLIK

FLIK is a spatial modulation scheme where each constellation point in the spatial domain corresponds to a particular combination of active LEDs. The number of activated LEDs, in general, is not fixed compared to space shift keying (SSK). A more general case of FLIK is called Flexible LED index modulation (FLIM) proposed in [10], where symbols can be encoded both in the spatial and signal domains.

Generally, the performance of a system based on FLIK strongly depends on the distinguishability of various active beam combinations. Each combination of active LED beams can be mapped to a corresponding irradiance incident at the receiver (in the case of a single receiver) or a combination of irradiances (in the case of multiple receivers). In this case, a pairwise Euclidean distance between two different active LED beam combinations corresponds to their mutual irradiance difference.

When a system consisting of many LED beams is considered, the selection of engaged beams (i.e. beams that can be activated during the symbol transmission) becomes a key determiner of the link performance. A fast beam selection method is required for optimal link performance in a dynamic use case scenario where the UE position and orientation can change rapidly. A good selection criterion for such a method is the maximal SNR criterion [12] as it only requires the estimation of individual channel SNR for each transmitter and receiver pair, evading the necessity of explicitly calculating the Euclidean distances for all symbols of all potential engaged beam combinations.

B. Rotational Geometry

It is well known that any arbitrary rotation in $\mathbb{R}^3$ space can be achieved by 3 successive elementary rotations about the axes of the coordinate system. Mathematically this is described by the multiplication of 3 elementary rotation matrices each around its respective axis [13]. The coordinate system about which the rotation is performed can be chosen to be local or global. We denote local coordinate system with xyz and the global with *XYZ* labels.

It is important to remember that the matrix multiplication is non-commutative; therefore, the order of elementary rotations is important; this leads to 6 different possible choices on the order of rotations for Euler angles. In this study, we will follow the world wide web consortium (WC3) specification [14]. Here, intrinsic rotation orders are $(z \rightarrow x' \rightarrow y'')$ here $x'y'z'$ and $x''y''z''$ are the local co-ordinate systems after rotation about z-axis followed by rotation about x'-axis. The elementary rotation angles in degrees are yaw $\alpha \in [0, 360)$ corresponding to the rotation around z-axis, pitch $\beta \in [-180, 180)$ corresponding to the rotation around x-axis and roll $\gamma \in [-90, 90)$ corresponding to the rotation around y-axis. The rotations are shown in Figure 1.

Using Euler's rotation theorem we can write any arbitrary rotation matrix as [13] $\mathbf{R}(\alpha, \beta, \gamma) = \mathbf{R}_\alpha \mathbf{R}_\beta \mathbf{R}_\gamma$. We denote a single i-th receiver (or j-th LED) normal vector aligned to the global co-ordinate system as $\mathbf{n}_i = [n_{1,i}, n_{2,i}, n_{3,i}]$, the rotated normal vector is given as $\mathbf{n'}_i = [n'_{1,i}, n'_{2,i}, n'_{3,i}]$. From the Euler's theorem the rotated normal vector can be expressed as: $\mathbf{n'}_i = \mathbf{R}(\alpha, \beta, \gamma)\mathbf{n}_i = \mathbf{R}_\alpha \mathbf{R}_\beta \mathbf{R}_\gamma \mathbf{n}_i$. The explicit form of the rotation matrix is given by (1). In this study we assume a fixed orientation of the AP. For the further convenience we will denote a general orientation as $\mathbf{\Omega} = \{\alpha, \beta, \gamma\}$ and $\mathbf{R}(\alpha, \beta, \gamma) = \mathbf{R}(\mathbf{\Omega})$.

C. FLIK System Description

A binary permutation vector $\mathbf{b}_k = [b_0, b_1, ...b_{N_{\mathrm{LED}}^{\mathrm{eng}}(\mathbf{r},\mathbf{\Omega})-1}]^{\mathrm{T}} \in \mathbb{B}(\mathbf{r}, \mathbf{\Omega})$ and $b_{i,k} \in \{0, 1\}$ is mapped one-to-one to a spatial domain symbol $\mathbf{x}_k = [x_0, x_1, ...x_{N_{\mathrm{LED}}^{\mathrm{eng}}(\mathbf{r},\mathbf{\Omega})-1}]^{\mathrm{T}} \in \mathbb{X}(\mathbf{r}, \mathbf{\Omega})$, $x_{i,k} \in \{0, P\}$ using a locally compiled mapping function $f_{\mathbb{X}(\mathbf{r},\mathbf{\Omega})} : \mathbf{b}_k \in \mathbb{B}(\mathbf{r}, \mathbf{\Omega}) \mapsto \mathbf{x}_k \in \mathbb{X}(\mathbf{r}, \mathbf{\Omega})$ and corresponding to a combination of activated LEDs. $\mathbb{B}(\mathbf{r}, \mathbf{\Omega})$ and $\mathbb{X}(\mathbf{r}, \mathbf{\Omega})$ are the set of binary permutation vectors and the symbol alphabet respectively, $N_{\mathrm{LED}}^{\mathrm{eng}}(\mathbf{r}, \mathbf{\Omega})$ - number of engaged LEDs, P - irradiated optical power from a single LED cell.

We note here that both the symbol alphabet, permutation vector set and mapping between them are functions of both position $\mathbf{r}$ and orientation $\mathbf{\Omega}$ that can vary rapidly with user movement.

The cardinality of the local symbol alphabet in FLIK is:

$$|\mathbb{X}(\mathbf{r}, \mathbf{\Omega})| = |\mathbb{B}(\mathbf{r}, \mathbf{\Omega})| = 2^{N_{\mathrm{LED}}^{\mathrm{eng}(\mathbf{r},\mathbf{\Omega})}} \tag{2}$$

$$\mathbf{R}(\alpha, \beta, \gamma) = \begin{bmatrix} \cos\alpha\cos\gamma - \sin\alpha\sin\beta\sin\gamma & -\sin\alpha\cos\beta & \sin\alpha\sin\beta\cos\gamma + \cos\alpha\sin\gamma \\ \cos\alpha\sin\beta\sin\gamma + \sin\alpha\cos\gamma & \cos\alpha\cos\beta & \sin\alpha\sin\gamma - \cos\alpha\sin\beta\cos\gamma \\ -\cos\beta\sin\gamma & \sin\beta & \cos\beta\cos\gamma \end{bmatrix} \tag{1}$$

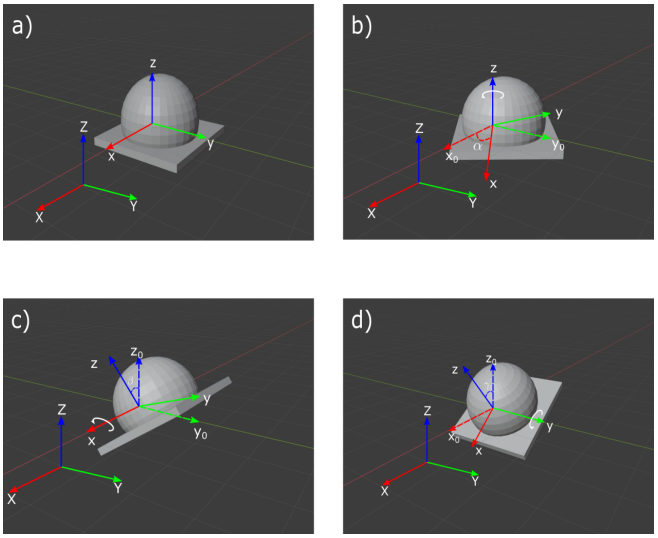

Fig. 1: Orientations of a hemisphere: a) aligned to global axes, b) yaw rotation with angle α, c) pitch rotation with angle β, d) roll rotation with angle γ

While in some cases it is possible that the number of engaged beams will be equal to all the LED cells in an AP, for a sufficiently large amount of beams the number of engaged beams $N_{\text{LED}}^{\text{eng}}(\mathbf{r},\mathbf{\Omega}) = |\mathbb{E}(\mathbf{r},\mathbf{\Omega})|$ will be typically smaller than the number of avaialble ones $N_{\text{LED}}^{\text{available}}(\mathbf{r},\mathbf{\Omega}) = |\mathbb{A}(\mathbf{r},\mathbf{\Omega})|$. The sets of engaged n_j an available m_j LEDs are given as: $\mathbb{E}(\mathbf{r},\mathbf{\Omega}) = \{n_0, n_1, ..., n_{N_{\text{LED}}^{\text{eng}}(\mathbf{r},\mathbf{\Omega})-1}\}$ n_j and $\mathbb{A}(\mathbf{r},\mathbf{\Omega}) = \{m_0, m_1, ..., m_{N_{\text{LED}}^{\text{available}}(\mathbf{r},\mathbf{\Omega})-1}\}$ and $\mathbb{E}(\mathbf{r},\mathbf{\Omega}) \subseteq \mathbb{A}(\mathbf{r},\mathbf{\Omega})$.

While so far we only discussed the selection transmitting side of the link, a similar problem applies for the receiver end when more than one receiver cell is considered.

The transmission over the MIMO channel for the selected beams is described by a $N_{\text{r}}(\mathbf{r},\mathbf{\Omega}) \times N_{\text{LED}}^{\text{eng}}(\mathbf{r},\mathbf{\Omega})$ dimension optical DC channel gain matrix [14]:

$$\mathbf{H}(\mathbf{r},\mathbf{\Omega}) = \begin{bmatrix} h_{11}(\mathbf{r},\mathbf{\Omega}) & \dots & h_{1N_{\text{LED}}^{\text{eng}}(\mathbf{r},\mathbf{\Omega})}(\mathbf{r},\mathbf{\Omega}) \\ \vdots & \ddots & \vdots \\ h_{N_{\text{r}}(\mathbf{r},\mathbf{\Omega})1}(\mathbf{r},\mathbf{\Omega}) & \dots & h_{N_{\text{r}}(\mathbf{r},\mathbf{\Omega})N_{\text{LED}}^{\text{eng}}(\mathbf{r},\mathbf{\Omega})} \end{bmatrix} \tag{3}$$

Here each matrix element $h_{ij}(\mathbf{r},\mathbf{\Omega})$ corresponds to an optical channel DC gain between engaged j^{th} LED and i^{th} receiver cells. The number of active receivers is $N_{\text{r}}(\mathbf{r},\mathbf{\Omega})$. The received signal vector is given by $\mathbf{y}(\mathbf{r}) = [y_0, y_1, ...y_{N_{\text{r}}(\mathbf{r})-1}]^{\text{T}} \in \mathbb{R}_{N_{\text{r}}^{\text{eng}}(\mathbf{r},\mathbf{\Omega})\times 1}$, where $\mathbf{y}$ is expressed from:

$$\mathbf{y}(\mathbf{r},\mathbf{\Omega}) = \mathbf{H}(\mathbf{r},\mathbf{\Omega})\mathbf{x}_k + \mathbf{n}(\mathbf{r},\mathbf{\Omega}) \tag{4}$$

Additive white Gaussian noise (AWGN) is described by $\mathbb{R}_{N_{\text{r}}(\mathbf{r},\mathbf{\Omega})\times 1}$ dimension vector $\mathbf{n}(\mathbf{r})$, the elements of the vector are distributed by $\mathcal{N}(0, \sigma_i^2(\mathbf{r},\mathbf{\Omega}))$, and $\sigma_i^2(\mathbf{r},\mathbf{\Omega}))$ with the variance given as:

$$\sigma_i^2(\mathbf{r},\mathbf{\Omega}) = N_{0,i}(\mathbf{r},\mathbf{\Omega})B \tag{5}$$

Here $N_{0,ij}(\mathbf{r},\mathbf{\Omega})$ is the single sided noise power spectral density, which is generally dependent on the UE location and orientation and B - denotes the one-sided spectral modulation bandwidth of the signal.

For the detection at the UE end the Maximum-Likelihood (ML) algorithm is used, the estimated data symbol $\hat{\mathbf{x}}_k$ is then given as:

$$\begin{aligned} \hat{\mathbf{x}}_k &= \arg \max_{\mathbf{x}_k \in \mathbb{X}(\mathbf{r},\mathbf{\Omega})} p_{\mathbf{y}}(\mathbf{y}(\mathbf{r},\mathbf{\Omega})|\mathbf{H}(\mathbf{r},\mathbf{\Omega})\mathbf{x}_k) \\ &= \arg \min_{\mathbf{x}_k \in \mathbb{X}(\mathbf{r},\mathbf{\Omega})} |\mathbf{y}(\mathbf{r},\mathbf{\Omega}) - \mathbf{H}(\mathbf{r},\mathbf{\Omega})\mathbf{x}_k|_{\text{F}}^2 \end{aligned} \tag{6}$$

The method based on the maximal SNR criterion where beam selector selects a set $\mathbb{E}(\mathbf{r},\mathbf{\Omega}) \subseteq \mathbb{A}(\mathbf{r},\mathbf{\Omega})$ that maximises the average electrical SNR γ of the link:

$$\Gamma_{\mathbb{E}(\mathbf{r},\mathbf{\Omega})} = \frac{1}{|\mathbb{E}(\mathbf{r},\mathbf{\Omega})|} \sum_{j \in \mathbb{E}(\mathbf{r},\mathbf{\Omega})}^{|\mathbb{E}(\mathbf{r},\mathbf{\Omega})|} \gamma_{ij}(\mathbf{r},\mathbf{\Omega}) \tag{7}$$

Compared to a more optimal method where the selection is based on maximising the total Euclidean distance of the D set.

$$D_{\mathbb{E}(\mathbf{r},\mathbf{\Omega})} = \sum_{k'=1}^{|\mathbb{X}(\mathbf{r},\mathbf{\Omega})|} \sum_{k=1}^{|\mathbb{X}(\mathbf{r},\mathbf{\Omega})|} \sqrt{d^2_{(\mathbf{x}_k,\mathbf{x}'_k)}} \tag{8}$$

$$= \sum_{k'=1}^{|\mathbb{X}(\mathbf{r},\mathbf{\Omega})|} \sum_{k=1}^{|\mathbb{X}(\mathbf{r},\mathbf{\Omega})|} |\mathbf{H}(\mathbf{r},\mathbf{\Omega})\Delta_{\mathbf{x}_k,\mathbf{x}_{k'}}|_{\text{F}} \tag{9}$$

Here $d(\mathbf{x}_k, \mathbf{x}'_k)$ - mutual Euclidean distance between symbol vectors and $\Delta_{\mathbf{x}_k,\mathbf{x}_{k'}}$ is defined as:

$$\Delta_{\mathbf{x}_k,\mathbf{x}_{k'}} = \mathbf{x}_k - \mathbf{x}_{k'} \tag{10}$$

III. Angle Diversity Hemispherical Transceiver Model

This section describes the design of an angle diversity hemispherical transceiver; an optical DC channel model will be given for a random position and orientation of the UE. The optical test setup and parameters will also be given in this section.

A. Hemispherical Transceiver MIMO-VLC Channel

The signal transmission over the LoS AWGN VLC channel for a given UE location $\mathbf{r}$ and orientation $\mathbf{\Omega}$ in the room is modelled by $N_{\text{r}}(\mathbf{r}) \times N_{\text{LED}}^{\text{eng}}(\mathbf{r})$ dimension optical direct-current (DC) channel gain matrix $\mathbf{H}(\mathbf{r},\mathbf{\Omega})$. Each matrix element $h_{ij}(\mathbf{r})$ corresponds to the mutual DC channel gain between i^{th} UE receiver cell and j^{th} AP LED cell and is given by [14]:

$$\begin{aligned} h_{ij}(\mathbf{r},\mathbf{\Omega}\lambda) = &\frac{m_{\text{lens}}+1}{2\pi d_{ij}^2(\mathbf{r})} A_{\text{PD}} G_{ij}^{\text{filter}}(\mathbf{r},\mathbf{\Omega}) G_{\text{con}} \\ &\times \cos^{m_{\text{lens}}}(\varphi_{ij}(\mathbf{r})) \cos(\psi_{ij}(\mathbf{r},\mathbf{\Omega})) \\ &\times \text{rec}\left(\frac{\psi_{ij}(\mathbf{r},\mathbf{\Omega})}{\Psi_c}\right) \end{aligned} \tag{11}$$

We have assumed that user orientation has a negligible effect on the distance $d_{ij}(\mathbf{r})$ between the AP and UE cells. Here $\psi_{ij}(\mathbf{r},\mathbf{\Omega})$ and φ_{ij} are given by the following expressions [15]:

$$\psi_{ij}(\mathbf{r},\mathbf{\Omega}) = \arccos\left(\frac{\mathbf{n'}_i \cdot \mathbf{d}_{ij}(\mathbf{r})}{d_{ij}(\mathbf{r})}\right)$$
$$\varphi_{ij}(\mathbf{r}) = \arccos\left(\frac{\mathbf{n}_j \cdot \mathbf{d}_{ij}(\mathbf{r})}{d_{ij}(\mathbf{r})}\right)$$

Here $\mathbf{n'}_i$ - UE receiver cell normal vector and $\mathbf{n}_j$ - AP LED cell vector. The LoS condition for the UE and AP cells is modelled as [15]:

$$\mathrm{rec}\left(\frac{\psi_{ij}(\mathbf{r},\mathbf{\Omega})}{\Psi_c}\right) = 1 \qquad \psi_{ij}(\mathbf{r},\mathbf{\Omega}) \leq \Psi_\mathrm{c}$$
$$\mathrm{rec}\left(\frac{\psi_{ij}(\mathbf{r},\mathbf{\Omega})}{\Psi_c}\right) = 0 \qquad \psi_{ij}(\mathbf{r},\mathbf{\Omega}) > \Psi_\mathrm{c}$$

Here Ψ_c is the acceptance angle of the compound parabolic concentrator (CPC). $G_{ij}^{\mathrm{filter}}(\mathbf{r},\mathbf{\Omega})$ – gain from the optical bandpass filter at the UE receiver cell, which is given as [16]:

$$G_{ij}^{\mathrm{filter}}(\mathbf{r},\mathbf{\Omega}) = T_{\mathrm{filter}}(\lambda_{ij}^{\psi}(\mathbf{r},\mathbf{\Omega}))$$

The filter transmissivity $T_{\mathrm{filter}}(\lambda_{ij}^{\psi}(\mathbf{r},\mathbf{\Omega}))$ is given at the angle of the beam incidence ψ against the surface normal vector of the filter. $\lambda_{ij}^{\psi}(\mathbf{r},\mathbf{\Omega})$ corresponds to the shifted central wavelength of the transmission passband [16]:

$$\lambda_{ij}^{\psi}(\mathbf{r},\mathbf{\Omega}) = \lambda\sqrt{(1-(\frac{n_0}{n_{\mathrm{filter}}})^2\sin^2\psi_{ij}(\mathbf{r},\mathbf{\Omega})}$$

Here n_0 - refractive index of the medium external to filter (we assume $n_0 = 1$). The refractive index of the optical bandpass filter is n_{filter} and λ is the shifted central wavelength of the passband. The photodetector's active area of a UE receiver cell is A_{PD}. In this study we will consider avalanche photodiodes for photodetectors. Lambertian order for the LEDs at the AP cell m_{LED} is given as [15]:

$$m_{\mathrm{LED}} = -\frac{\ln 2}{\ln(\cos(\Phi_{1/2}))}$$

Where $\Phi_{1/2}$ - half intensity angle of LEDs in the cell. The gain G_{con} is [14]:

$$G_{\mathrm{con}} = \frac{n^2}{\sin^2\Psi_\mathrm{c}}$$

Where n – refractive index of the UE receiver cell CPC.

The photocurrent generated by a UE cell by the irradiance from the jth AP LED cell for a given UE location and orientation can be written as [17]:

$$I_{ij}(\mathbf{r},\mathbf{\Omega}) = P_{\mathrm{opt}}^{\mathrm{lens}}(B)h_{ij}(\mathbf{r},\mathbf{\Omega})R(\lambda,B)M \tag{12}$$

With avalanche photo-diode responsivity $R(\lambda,B)$ and multiplication factor M. The optical power $P_{\mathrm{opt}}^{\mathrm{lens}}(B)$ is given at the output surface from condenser lens of the APC cell [18]:

$$P_{\mathrm{opt}}^{\mathrm{lens}}(B) = \frac{(m_{\mathrm{LED}}+1)D_{\mathrm{lens}}^2}{8d'^2}T_{\mathrm{lens}}P(B) \tag{13}$$

Where D_{lens} is the condenser lens diameter and d - distance between array of micro-LEDs and the condenser lens. The transmissivity of the lens is given as: $T_{\mathrm{lens}}(\lambda)$. The half intensity angle of the condenser lens is given as [18]:

$$\Phi_{1/2}^{\mathrm{lens}} = \frac{D_{\mathrm{LED}}}{2d'}$$

Here D_{LED} - diameter of the LED array. The Lambertian order of the beam at the output surface of the lens then can be simply expressed as:

$$m_{\mathrm{lens}} = -\frac{\ln 2}{\ln(\cos(\Phi_{1/2}^{\mathrm{lens}})}$$

Which is then used in (11):

After the opto-electrical conversion, the received electrical power is [17]:

$$P_{ij}^{\mathrm{elec}}(\mathbf{r}) = \frac{I_{ij}^2(\mathbf{r})G_{\mathrm{TIA}}^2}{R_{\mathrm{Load}}} \tag{14}$$

G_{TIA} - is the transimpedance amplifier (TIA) gain and R_{Load} - the receiver's load resistance.

The electrical signal-to-noise (SNR) for the signal incident at i^{th} UE receiver cell from j^{th} AP cell γ_{ij} can be expressed as [17]:

$$\gamma_{ij}^{\mathrm{elec}}(\mathbf{r}) = \frac{P_{ij}^{\mathrm{elec}}(\mathbf{r})}{\sigma_{ij}^2(\mathbf{r})} \tag{15}$$

In a well lit use case scenario, the primary source of the noise can be assumed to be due to the background illumination shot noise, which can be expressed as [17]:

$$\sigma_{ij}^2(\mathbf{r},\mathbf{\Omega}) = 2qM^2FR(\lambda,B)BI_{\mathrm{bg}}(\mathbf{r},\mathbf{\Omega})A_{\mathrm{PD}}\frac{G_{\mathrm{TIA}}^2}{R_{\mathrm{Load}}} \tag{16}$$

Here F - excess noise factor of an APD and I_{bg} - irradiance incident at the ith UE cell from the background source.

B. Optical Test Setup

The use case scenario is a well lit a $4\times4\times3\,\mathrm{m}^3$ office, with the AP fixed on the centre of the ceiling. The UE is considered to be near the floor and is free to move around the xy-plane of the room as well and have random orientation against the global XYZ axes. In this paper, we assume a dynamic walking scenario with the Gaussian orientation statistics from [19] shown in Table I.

The receiver cells and LED cells are uniformly distributed around their respective hemispheres. On the AP end, there are 41 LED cells. Each cell consists of a blue GaN micro-LED array from [20]. The maximum optical power of a single array $P_{\mathrm{array}} = 10\,\mathrm{mW}$ and half-intensity angle $\Phi_{1/2} = 60°$. Each LED cell consists of ten of these arrays; the arrays are

TABLE I: UE Orientation Statistics In Degrees from [19]

Angle	Mean	Standard deviation
Yaw α	-90	10
Pitch β	28.81	3.26
Roll γ	-1.35	5.42

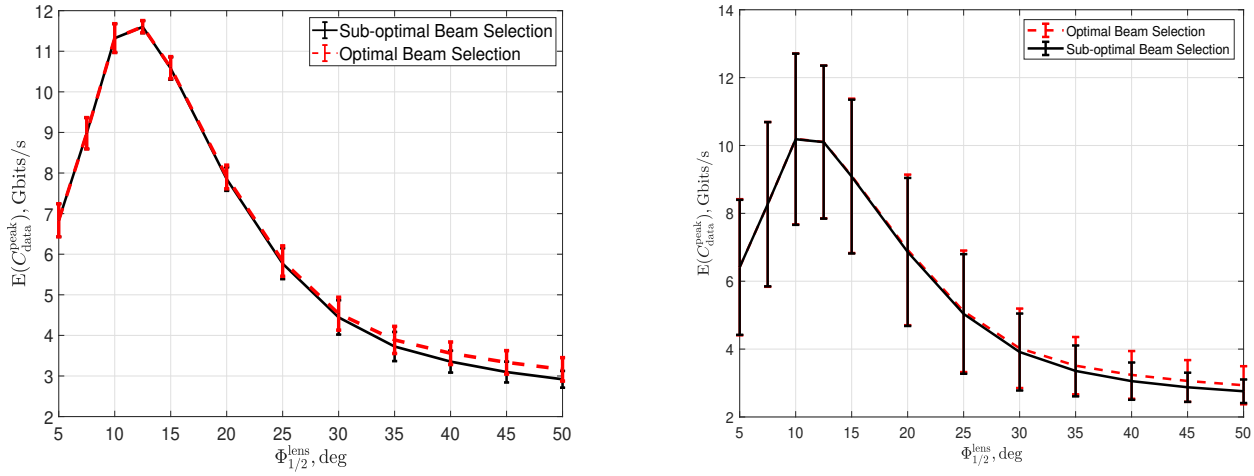

(a) (b)

Fig. 2: Mean data throughput for fast beam selection method (denoted as sub-optimal) and Euclidean distance based beam selection (denoted as optimal) for various $\Phi_{1/2}^{\mathrm{lens}}$ with a) fixed UE orientation, b) random UE orientation. The error bars indicate the standard deviation of the data throughput.

considered to be connected in parallel. A condenser lens is placed and aligned on the optical axis of the cell at a distance d. We leave the selection of the parameters of the condenser lens as variable, so that the intensity and FOV can be adjusted to explore the effect of various FOVs, furthermore, we set $P_{opt}^{\mathrm{lens}}(B)/P(B) = 10$. We assume that all micro-LED arrays are biased to produce the maximum output optical power.

On the UE end, and is the same for the AP case, there are 41 receiver cells. Each cell contains 25×25 array of Si-APDs (Hamamatsu Si APD S12023), the array is positioned at the output surface of the CPC (4.34 mm Output dia Compound parabolic concentrator (Edmundoptics)), while a blue band-pass filter (450 nm CWL, 25 mm dia. hard-coated OD 4.0 50 nm bandpass filter (Edmundoptics)) is placed at the input of the CPC.

We model the background illumination by assuming a 250 lux illumination, which is generated by 4 light sources at the positions $\{x, y, z\} = \{-1, -1, 3\}$ m, $\{-1, 1, 3\}$ m, $\{1, -1, 3\}$ m, $\{1, 1, 3\}$ m. Each light source produces a luminous flux of 1000 lumens with 3000 K colour illumination temperature. The spectrum is taken from [21]. The selection of the illumination and colour temperatures are selected in compliance with the office work conditions set out in [22]. We note that the background illumination far exceeds the signal in terms of luminous flux, which even at peak number of active LEDs would have contribution in order of tens of lumens rendering the effect of varying number of on-state LEDs marginal to the overall illumination of the office.

The spectral efficiency of the link at the UE position $\mathbf{r}$ and orientation $\mathbf{\Omega}$ is given as:

$$\eta(\mathbf{r}, \mathbf{\Omega}) = \log_2 |\mathbb{X}(\mathbf{r}, \mathbf{\Omega})| = N_{\mathrm{LED}}^{\mathrm{eng}}(\mathbf{r}, \mathbf{\Omega}), \eta(\mathbf{r}, \mathbf{\Omega}) \in \mathbb{N} \quad (17)$$

To calculate the achievable data throughput we assume forward error correction coding (FEC) at bit error ratio (BER) threshold of 3.8×10^{-3} and 7% [23] overhead, the maximum locally achievable data throughput for a given bandwidth B is:

$$C_{\mathrm{peak}}(\mathbf{r}, \mathbf{\Omega}, B) = 1.86\eta(\mathbf{r}, \mathbf{\Omega})B \quad (18)$$

IV. Computer Simulation Results and Analysis

In the following section, we present the mean peak achievable data throughput for a random user orientation following the statistics from Table I. The Monte-Carlo simulations are performed for 10^7 realisations of random UE orientation and position. The comparison between the maximal SNR and Euclidean distance criterion is shown in Figures 2a and 2b for various LED cell FOVs. The results are compared to the special fixed orientation case in Figure 2a where both AP and UE hemisphere normal vectors at the nadir and zenith are aligned with the global z-axis.

As can be seen from Figure 2b, for narrow enough half-intensity angles of AP cells, the achievable data throughput difference between the two methods is negligible. Furthermore, while the introduction of random orientation causes a decrease in the achievable mean data throughput compared to the fixed orientation case, it does not significantly affect the relative performance in terms of achievable mean data throughput between the two criteria.

In Figure 3 the difference between the two methods is given as:

$$\delta = \frac{\mathrm{E}(C_{\mathrm{data,Euclidean}}^{\mathrm{peak}}) - \mathrm{E}(C_{\mathrm{data,SNR}}^{\mathrm{peak}})}{\mathrm{E}(C_{\mathrm{data,Euclidean}}^{\mathrm{peak}})} \cdot 100\% \quad (19)$$

We note here that the relative difference between the two methods increases with the increasing half-intensity angle for

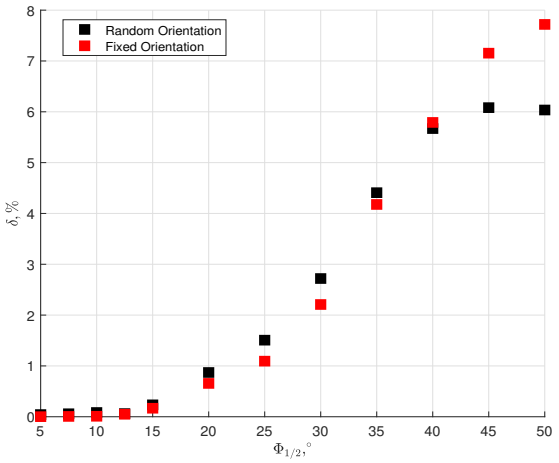

Fig. 3: Relative difference of mean data throughput between two methods various $\Phi_{1/2}^{\text{lens}}$ for fixed and random UE orientation.

both fixed and random orientations. However, the difference between methods in the case of random orientation reaches its peak value at significantly lower angles and smaller values. This can be attributed to an overall worse selection performance when random angles are considered, leading to smaller selected sets bridging the gap between two methods (there is no difference between two criteria when only one beam is considered for selection).

V. Conclusion and Outlook

In this paper, the performance of beam selection based on the maximal SNR criterion was investigated in an angle diversity hemispherical transceiver system using FLIK. The selection was compared to the method based on the maximal Euclidean distance selection. It was found that for beams that are narrow enough, the performance in the achievable data throughput is nearly identical between both criteria in such systems. However, the SNR based selection would only require $N_{\text{r}} \times N_{\text{LED}}^{\text{available}}$ SNR estimations while the beam selection based on the Eulcidean distance would require to estimate symbol distances for $\binom{N_{\text{LED}}^{\text{available}}}{N_{\text{LED}}^{\text{eng}}}$ beam combinations. Therefore, the SNR based selection method in angle diversity MIMO systems using FLIK require significantly less estimation operations while providing a comparable data throughput to the method based on the Euclidean distance. These results motivate further research of such MIMO systems for mobile use case scenarios where fast channel estimation can enable the use and development of more energy efficient allocation and handover methods of locally available pool of transmitters and receivers at a given time instant.

Acknowledgment

The authors acknowledge the ENLIGHT'EM project (H2020-MSCA ITN-2018 n. 814215) for the fundamental support in this research.

References

[1] Ericsson, 2021. Mobile data traffic outlook. [Online] Available at: https://www.ericsson.com/en/mobility-report/dataforecasts/mobile-traffic-forecast [Accessed 1 September 2021].

[2] Enerdata, 2020. Between 10 and 20% of electricity consumption from the ICT* sector in 2030?. [Online]

[3] Jones, N., 2018. How to stop data centres from gobbling up the world's electricity. *Nature*, 561(7722), pp.163-167.

[4] H. Burchardt, N. Serafimovski, D. Tsonev, S. Videv and H. Haas, "VLC: Beyond point-to-point communication," in *IEEE Communications Magazine*, vol. 52, no. 7, pp. 98-105, July 2014.

[5] H.Haas, L.Yin, Y.Wang, and C.Chen, "What is LiFi?," *J. Lightwave Technol*, vol. 34, 1533-1544, 2016.

[6] L. Kong, C. Chen, Y. Wang and H. Haas, "Power Consumption Evaluation in High Speed Visible Light Communication Systems," *2018 IEEE Global Communications Conference (GLOBECOM)*, Abu Dhabi, United Arab Emirates, 2018, pp. 1-6.

[7] E. Telatar, "Capacity of multi-antenna Gaussian channels," *Eur. Trans*. Telecommun., vol. 10, no. 6, pp. 585–595, 1999.

[8] R. Y. Mesleh, H. Haas, S. Sinanovic, C. W. Ahn and S. Yun, "Spatial Modulation," in *IEEE Transactions on Vehicular Technology*, vol. 57, no. 4, pp. 2228-2241, July 2008, doi: 10.1109/TVT.2007.912136.

[9] J. Jeganathan, A. Ghrayeb and L. Szczecinski, "Generalized space shift keying modulation for MIMO channels," *2008 IEEE 19th International Symposium on Personal, Indoor and Mobile Radio Communications*, 2008, pp. 1-5, doi: 10.1109/PIMRC.2008.4699782.

[10] A. Yesilkaya, A. A. Purwita, E. Panayirci, H. V. Poor and H. Haas, "Flexible LED Index Modulation for MIMO Optical Wireless Communications," *GLOBECOM 2020 - 2020 IEEE Global Communications Conference*, 2020, pp. 1-7, doi: 10.1109/GLOBECOM42002.2020.9322528.

[11] R. Rajashekar, K. V. S. Hari and L. Hanzo, "Antenna Selection in Spatial Modulation Systems," in *IEEE Communications Letters*, vol. 17, no. 3, pp. 521-524, March 2013, doi: 10.1109/LCOMM.2013.012213.122650.

[12] M. Gharavi-Alkhansari and A. B. Gershman, "Fast antenna subset selection in MIMO systems," in *IEEE Transactions on Signal Processing*, vol. 52, no. 2, pp. 339-347, Feb. 2004, doi: 10.1109/TSP.2003.821099.

[13] J. B. Kuipers, Quaternions and Rotation Sequences: *A Primer With Applications to Orbits, Aerospace and Virtual Reality*, vol. 66. Princeton, NJ, USA: Princeton Univ. Press, 1999

[14] World Wide Web Consortium (W3C). (Jul. 2016). *Device Orientation Event Specification*. [Online]. Available: https://specification at w3c.github.io

[15] J. M. Kahn and J. R. Barry, "Wireless infrared communications," in *Proceedings of the IEEE*, vol. 85, no. 2, pp. 265-298, Feb. 1997, doi: 10.1109/5.554222.

[16] J. R. Barry and J. M. Kahn, "Design of non-directed infrared links for high-speed wireless networks," *Proceedings of LEOS'94*, 1994, pp. 207 vol.1-, doi: 10.1109/LEOS.1994.586965.

[17] S.Dimitrov and H.Haas, *Principles of LED light communications: towards networked Li-Fi*. Cambridge, UK: Cambridge University Press, 2015.

[18] J. Fakidis, M. Ijaz, S. Kucera, H. Claussen and H. Haas, "On the design of an optical wireless link for small cell backhaul communication and energy harvesting," *2014 IEEE 25th Annual International Symposium on Personal, Indoor, and Mobile Radio Communication (PIMRC)*, 2014, pp. 58-62, doi: 10.1109/PIMRC.2014.7136132.

[19] M. Dehghani Soltani, A. A. Purwita, Z. Zeng, C. Chen, H. Haas and M. Safari, "An Orientation-Based Random Waypoint Model for User Mobility in Wireless Networks," *2020 IEEE International Conference on Communications Workshops (ICC Workshops)*, 2020, pp. 1-6, doi: 10.1109/ICCWorkshops49005.2020.9145333.

[20] E. Xie et al., "Over 10 Gbps VLC for Long-Distance Applications Using a GaN-Based Series-Biased Micro-LED Array," in *IEEE Photonics Technology Letters*, vol. 32, no. 9, pp. 499-502, 1 May1, 2020, doi: 10.1109/LPT.2020.2981827.

[21] LSPDD: Lamp Spectral Power Distribution Database, LED GE A19 Domestic, October 2012. Accessed on: August 18, 2021. [Online]. Available: https://lspdd.org/app/en/lamps/2595

[22] Health and Safety Executive (HSE), *Lighting at Work*, 2nd ed.Sudbury, Suffolk: HSE Books, 1997.

[23] ITU-T, "Forward error correction for high bit-rate dwdm submarine systems," Apr 2005. [Online]. Available: https://www.itu.int/rec/ T-REC-G.975.1-200402-I/en